THE JOURNAL OF PHYSICAL CHEMISTRY C

Article

pubs.acs.org/JPCC

# Adsorption and Dissociation of $CO_2$ on Ru(0001)

M. Pachecka, J. M. Sturm, C. J. Lee,* and F. Bijkerk

Industrial Focus Group XUV Optics, MESA+ Institute for Nanotechnology, University of Twente, Drienerlolaan 5, Enschede, The Netherlands

**ABSTRACT:** The adsorption and dissociation of carbon dioxide on a Ru(0001) single crystal surface was investigated by reflection−absorption infrared spectroscopy (RAIRS) and temperature-programmed desorption (TPD) spectroscopy for $CO_2$ adsorbed at 85 K. RAIRS spectroscopy shows that the adsorption of $CO_2$ on a Ru(0001) single crystal is partially dissociative, resulting in $CO_2$ and CO. The CO vibrational mode was also observed to split into two distinct modes, indicating two general populations of CO present at the surface. Furthermore, a time-dependent blue-shift is observed, which is characteristic of increasing CO surface coverage. TPD showed that coverages of up to 0.3 ML were obtained, and no evidence for chemisorption of oxygen on ruthenium was found.

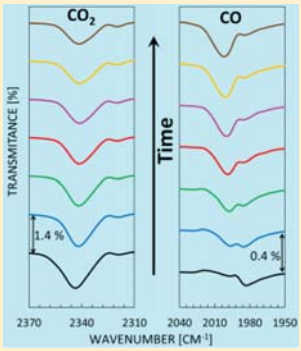


## 1. INTRODUCTION

The transformation of carbon dioxide ($CO_2$) into more valuable compounds (carbon monoxide, methanol, oxalate, organic acids, methane, hydrocarbons) requires activation by a catalyst.[1] Among ionic liquids, proteins, organic compounds, and semiconductors,[2] transition metals are studied widely as catalysts, due to their relatively high efficiency. Thus, the interaction of $CO_2$ with metal and metal oxide surfaces is of importance in understanding a number of relevant surface catalytic processes on an atomic scale.[1,3,4]

The reaction of $CO_2$ dissociation products with hydrogen to produce hydrocarbons is attractive as a potential net-zero emissions fuel cycle. However, for such a cycle to be efficient, the catalysis of $CO_2$ dissociation and the reverse water gas shift reaction is required. While metallic ruthenium is known to catalyze the reverse water gas shift reaction, its interaction with $CO_2$ has not, to our knowledge, been the subject of investigation.[5−8] The chemisorption and reaction of $CO_2$ on metal oxides, including $RuO_2$, and metallic alloys, including Ru, are well-studied processes.[1,3] Moreover, the adsorption of $CO_2$ on other single-crystal metal surfaces has been extensively studied. For surfaces like Fe, Ni, Re, Al, or Mg, it was observed that the adsorption of $CO_2$ is partially dissociative, with $CO_2$ decomposing to CO and O.[9−13] The dissociation of $CO_2$ proceeds via the formation of negatively charged $CO_2^-$ on Ni, Fe, Cu, and Re, which may then dissociate into CO and O.[1]

These experiments are often complicated by the low desorption temperature of $CO_2$. In many cases (Rh, Pd, Pt, Fe, Cu, Re) $CO_2$ does not stably adsorb to the surface for temperatures above 100 K, and desorbs from the surface for temperatures that are relatively low: 130 K (Re) and 135 K (Pd), with Ni being an exception at 220 K.[1] Additionally, surface purity is a very important factor in $CO_2$ adsorption and reaction on metals. Alkali adatoms, for example, increase the binding energy of adsorbed $CO_2$ and promote the partial dissociation of $CO_2$ into CO + O.

Many surface studies have been performed using scanning tunneling microscopy (STM), low energy electron diffraction (LEED), and X-ray photoelectron spectroscopy (XPS). STM provides valuable insight into the morphology and short-range order of surface adsorbed species;[14−16] however, it can be challenging to resolve some chemical reactions, such as partial dissociation ($CO_2 \rightarrow CO + O$). LEED is sensitive to ordered overlayer structures, and XPS is sensitive to chemical changes at the surface, but the relatively high energy of the electron and X-ray irradiation can lead to surface modifications that may be difficult to separate from the changes of interest.[17−22]

TPD studies, however, provide a direct measurement of the surface binding energy and allow the surface coverage to be absolutely calibrated. RAIRS measurements allow the growth and decay of vibrational modes to be studied in situ. These changes provide evidence for changes in molecular population density, molecular orientation, and the environment in which molecules are adsorbed to the surface. By combining TPD and RAIRS, it is often possible to draw quantitative conclusions that would be otherwise elusive. Moreover, due to the low energy of the radiation in RAIRS, in situ studies are highly unlikely to modify the surface during measurement.

In this article, we present the results of TPD and RAIRS studies of $CO_2$ adsorption and dissociation on a Ru(0001) single crystal surface at 85 K. Additionally, the behavior of the adsorbed species after increasing the surface temperature to 120 K was studied.

## 2. METHODS

A ruthenium (0001) single crystal with a diameter of 11 mm and thickness of ∼3 mm (Surface Preparation Laboratories, The Netherlands) was used for $CO_2$ adsorption and dissociation studies.

**Received:** January 2, 2017
**Revised:** March 2, 2017
**Published:** March 3, 2017





DOI: 10.1021/acs.jpcc.7b00021
J. Phys. Chem. C XXXX, XXX, XXX−XXX

The sample was mounted on a 3-axis positioning manipulator in an ultrahigh vacuum (UHV) chamber with a base pressure of $10^{-10}$ mbar. The temperature of the sample was controlled by a Eurotherm temperature controller with active heating and liquid nitrogen cooling. A K-type thermocouple was spot-welded to the side of the crystal and used to monitor the sample temperature.

The system was equipped with facilities for TPD and RAIRS measurements. A Hiden Analytical 3F/PIC quadrupole mass spectrometer (QMS) was used for thermal desorption measurements. To ensure that the signal was dominated by desorption from the crystal surface, the QMS was mounted inside a differentially pumped housing which was placed approximately 1 mm from the crystal surface during measurements. TPD measurements were performed by heating the crystal surface at a constant rate of 2 K/s in the range 85−600 K and at a rate of 10 K/s from 600 to 1580 K. For RAIRS measurements, a Bruker Vertex 70v Fourier transform infrared (FTIR) spectrometer, employing a liquid nitrogen cooled mercury−cadmium−telluride (MCT) detector was used. Background and sample scans were recorded by coadding 256 scans with a resolution of 4 $cm^{-1}$.

The crystal surface was subjected to a cleaning process, consisting of oxygen cleaning, annealing, and Ar ion sputtering. In the first step, carbon was removed by sample oxidation at 1300 K with an $O_2$ background pressure of $1 \times 10^{-7}$ mbar. Afterward, Ar ion sputtering (2 keV), with an argon pressure of $2 \times 10^{-6}$ mbar was performed. Finally the sample was annealed at 1300 K and flashed to 1580 K. Sputtering and annealing were repeated until no carbon monoxide peak was observed on the TPD spectrum and until a repeatable water TPD spectrum was achieved.[23]

Carbon dioxide, with a purity of 99.998% (residual gases: $O_2$ 2 ppm, $N_2$ 8 ppm, hydrocarbons 3 ppm, $H_2O$ 1 ppm, CO 1 ppm) was used for the experiments. Carbon dioxide was dosed on the Ru(0001) surface, held at a temperature of 85 K, using a retractable quartz dosing tube, placed 1 cm from the crystal to minimize the increase in the background pressure. A pinhole was mounted between the gas supply and the tube doser, such that a pressure in the mbar range in the dosing system results in effective pressures in the $10^{-8}$ mbar range in front of the crystal surface. The relatively high pressure in the dosing system minimizes possible contaminations from walls of the gas lines. Since $CO_2$ does not stably adsorb at the lowest achievable temperature of 85 K, calibration of the dose is not straightforward. Therefore, gas doses are specified as pressure used in the dosing system times exposure time. The surface coverage, which is the more important parameter, is determined by calibrating the total amount of $CO_2$ detected via TPD against reference water TPD spectra (see section 3.3 for details).

It is known that $CO_2$ adsorption on metal surfaces strongly depends on dosing time, pressure, surface temperature, and presence of contaminants on the surface.[1] This results in some additional uncertainty in the initial coverage for identical dosing conditions. To avoid incorporating this uncertainty into our study, we draw quantitative results from time-series data taken from the same experiment, rather than comparing between experiments.

## 3. RESULTS AND DISCUSSION

**3.1. $CO_2$ Adsorption on Ru(0001).** To ensure that all vibrational features were clearly identified, RAIRS spectra were first obtained from a Ru(0001) surface that was dosed with a large amount (dosing pressure approximately 5 mbar for less than 1 min) of $CO_2$ (see Figure 1). Five dominant vibrational modes were detected at frequencies that correspond closely to

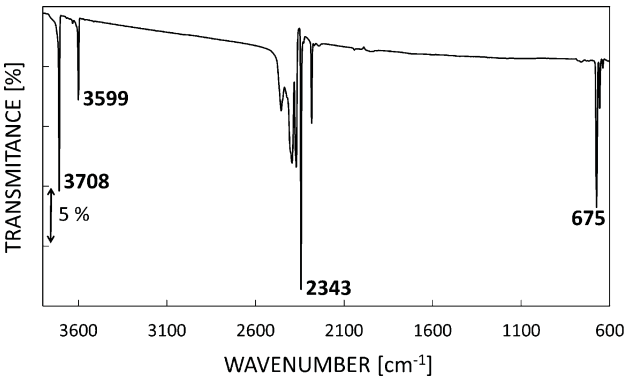


**Figure 1.** Reflection−absorption infrared spectrum of $CO_2$ adsorbed on Ru(0001) at 85 K.

those reported in literature, and their attributions are summarized in Table 1.[24,25] The only exception is the feature at

**Table 1. Assignment of RAIRS Peaks of $CO_2$/Ru(0001) from ref 24[a].**

| peak ($cm^{-1}$) | assignment |
|---|---|
| 3708 | ($\nu_1 + \nu_3$) combination |
| 3599 | ($2\nu_2 + \nu_3$) combination |
| 2343 | ($\nu_3$)[12] C═O stretch |
| 675 | ($\nu_2$) O═C═O bend |

[a] $\nu$ indicates a stretch vibration, with $\nu_1$ for symmetric and $\nu_3$ for asymmetric stretch.

675 $cm^{-1}$, which we attribute to the ($\nu_2$) O═C═O bending mode, but we note that this is more commonly reported to be at 660 $cm^{-1}$.[24,26,27] As shown in Figure 1, the peak at 2343 $cm^{-1}$ is broadened and several separate peaks between 2283 and 2455 $cm^{-1}$ are observed. Such broadening is common for thick layers and especially for layers that are interacting with a substrate.[25] In the following experiments, much less than a monolayer of $CO_2$ was dosed (1, 2, and 3 mbar) and only the $v_3$ stretch (2343 $cm^{-1}$) and ($\nu_2$) O═C═O bending mode (675 $cm^{-1}$) were observed. These vibrational modes consist of a single peak each, in line with previous literature reports. The center frequency of the two modes did not change for different $CO_2$ coverages. Taken together with the consistent shape of the TPD spectra for different coverages, we conclude that the structure of the adsorbed $CO_2$ does not change significantly in this coverage range.

$CO_2$ adsorption on Ru(0001) surface was additionally studied with TPD. Carbon dioxide already starts desorbing from the Ru(0001) surface at 85 K; moreover, the desorption peak is rather broad and extends beyond 120 K (see Figure 2), and thus, we expect some of the $CO_2$ to desorb from the surface during dosing

To exclude the influence of the instability of $CO_2$ on our measurements, we dose $CO_2$ for 10 min with different pressures (1, 2, and 3 mbar) in the dosing system, which corresponds to different surface coverage (0.05, 0.2, and 0.3 of a ML, respectively) of $CO_2$. The surface coverage was estimated using a reference water TPD spectrum for calibration purposes. Based on the water TPD,[28] we can estimate water coverage, and then


DOI: 10.1021/acs.jpcc.7b00021
J. Phys. Chem. C XXXX, XXX, XXX−XXX

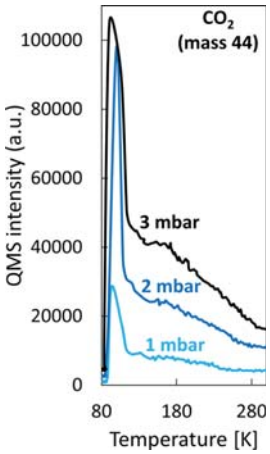


**Figure 2.** Desorbed peaks of $CO_2$ from TPD measurement after $CO_2$ dosed at 85 K onto the surface for 10 min with different pressures in the dosing system (1, 2, and 3 mbar).

taking into account the sensitivity of the mass spectrometer we calculated amount of CO, $CO_2$, and $H_2$ (section 3.3) on the

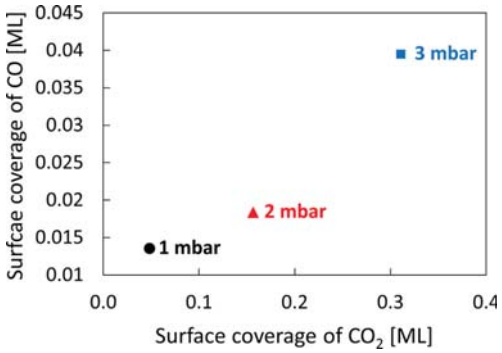


**Figure 3.** Surface coverage of CO as a function of $CO_2$ dosed onto the Ru(0001) surface in the pressure of 1, 2, and 3 mbar.

surface. After dosing, the two main contributions to the TPD spectrum are $CO_2$ (at 105 K) and CO (at 480 K). Figure 3 shows the relation between the CO observed at the surface and the $CO_2$ dosed onto the surface. Carbon dioxide and CO surface coverages are below 1 ML; thus, we expect dose-dependence coverage. As we will show later, the surface coverage of CO is clearly above the measured background (see Figure 9 for comparison) and depends on the $CO_2$ dose.

**3.2. $CO_2$ Dissociation on Ru(0001).** To study the rate at which $CO_2$ partially dissociates on the Ru(0001) surface, $CO_2$ was dosed onto the surface for 10 min at a pressure of 1 mbar, after which the surface was monitored with RAIRS for 50 min (including dosing time). Directly after that, the sample surface was heated to 120 K, and RAIRS measurements were obtained after cooling to 85 K. The change in the CO and the $CO_2$ ($\nu_3$ stretch and $\nu_2$ O═C═O bend modes) over time is presented in Figure 4a,b.

To quantify the changes in $CO_2$ and CO coverage, the intensity of the asymmetric stretching modes of $CO_2$ and CO were used, although it should be noted that RAIRS spectra are generally not quantitative. Figure 4 shows that the $CO_2$ $\nu_3$ mode slowly decreases with time; moreover, it is also red-shifted from 2343 to 2341 $cm^{-1}$. For low coverages of CO, like those used in this work, it is known that intensity of the asymmetric stretch

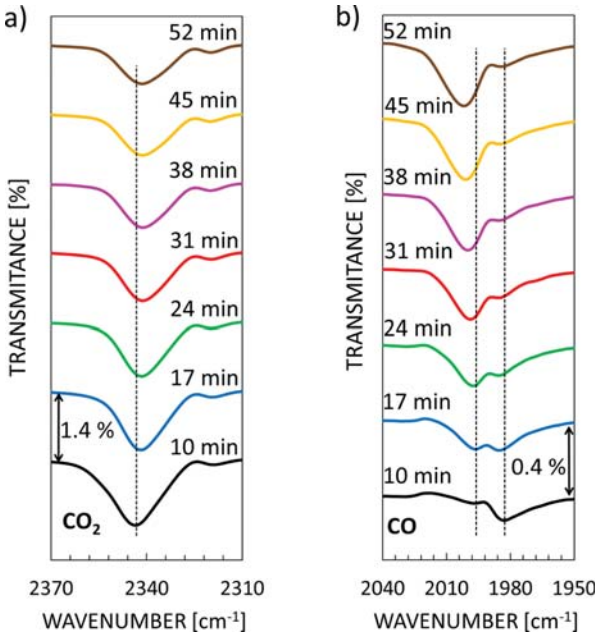


**Figure 4.** Reflection−absorption infrared spectrum of $CO_2$ stretch mode (a) and CO (b) for different delay times, after dosing $CO_2$ onto a Ru(0001) surface at 85 K. Dashed lines indicate the peak positions for 10 min measurement at 85 K.

mode scales approximately with coverage;[29] thus, we assume that all the changes in the spectra are due to changes in coverage. Our analysis shows that the intensity changes correspond to a reduction in $CO_2$ coverage from 0.05 to 0.03 ML, as shown in Figure 5. Moreover, it can be seen that approximately half of the

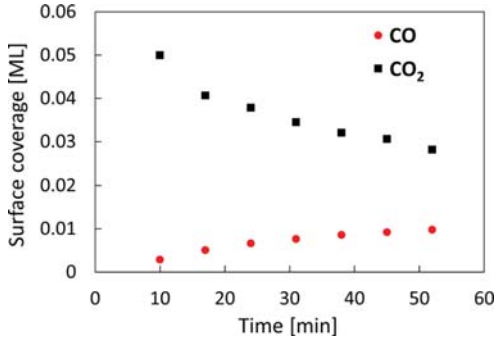


**Figure 5.** Integrated area of the CO and $CO_2$ ($v_3$ stretch mode) peaks converted into ML coverage after dosing onto Ru(0001) surface. Numbers are just indicative.

$CO_2$ loss is due to desorption from the surface, and the remaining loss is due to dissociation into CO. Similar behavior was observed in $CO_2$ adsorption on Ni(100) studies,[10,11,30] where it was shown that adsorption of $CO_2$ (100 L) on Ni(100) results in $CO_2$ and CO desorption from the surface. Based on evidence from EELS experiments, the existence of a "bent" $CO_2$ configuration was proposed as a precursor to dissociative adsorption. A vibrational mode at 1620 $cm^{-1}$ was assigned to an asymmetric stretching mode of a bent $CO_2$ species, while peaks at 670 and 2350 $cm^{-1}$ originate from the vibrational modes of linear, undistorted $CO_2$.

Although the presence of peaks at 660 and 2343 $cm^{-1}$ was observed after adsorption of $CO_2$ on Ru(0001), no evidence for a vibrational mode at 1620 $cm^{-1}$ was found. Only after increasing



DOI: 10.1021/acs.jpcc.7b00021
J. Phys. Chem. C XXXX, XXX, XXX−XXX

the dose and flux of $CO_2$, by using a higher dosing pressure, a mode at 1580 $cm^{-1}$ was detected. We speculate that this mode may be due to the asymmetric stretch of distorted $CO_2$, but we cannot definitively assign it. Due to the low amounts of CO formed on Ru(0001) and the reported instability of bent $CO_2$, the coverage of this species might be too low to be reliably detected. Transition metals with full d-band are known to be less active than metals with unpaired d-electrons; thus, dissociative adsorption is more likely on Ru, as evidenced by the reported behavior of $CO_2$ on Fe, Ni, and Re.[1,31] In contrast, $CO_2$ does not partially dissociate on evaporated Cu films at 195 and 273 K, as well as on Cu(110) and Cu(111) surfaces, which was attributed to the full d-bands.[1]

The CO vibrational mode, however, shows a more complicated behavior. The single vibrational mode splits into two. The higher energy mode consistently increases with time, and blue-shifts from 1996 to 2002 $cm^{-1}$ as the amount of CO increases.[29] At the same time, the lower energy mode (at 1983 $cm^{-1}$) does not grow consistently, but first increases and then decreases. The peak is first blue-shifted to 1986 $cm^{-1}$, then red-shifts to 1985 $cm^{-1}$ (see Figure 4 for a comparison). To distinguish the changes in intensity of these modes, the peaks (including $CO_2$ stretch mode) were fit with Gaussians, and the changes in areas of the peaks are presented in Figure 6.

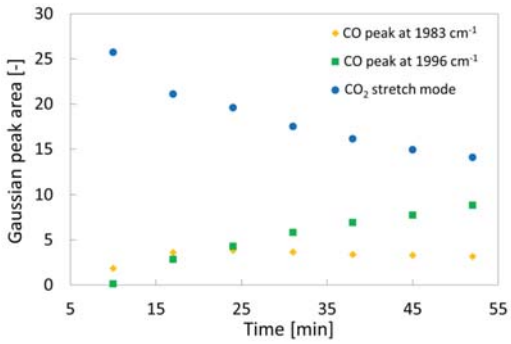


**Figure 6.** Peak areas after fit with Gaussians for $CO_2$ stretch mode and two CO modes, after 10 min $CO_2$ dose at 1 mbar.

It can be seen in Figure 6 that the area of the lower energy CO mode first increases and afterward saturates, or even slowly decreases. However, the higher energy CO mode increases as the $CO_2$ mode decreases. These spectral changes suggest that there are two CO populations. There are a number of possible explanations for the splitting of the vibrational mode: there may be two different binding energies, due to CO binding at two different sites. One site could be associated with nearby $CO_2$, while the other is associated with CO that is not associated with $CO_2$. Another possible explanation is that the dissociation of $CO_2$ results in chemisorbed oxygen with the CO vibrational frequency shifted due to its proximity. A final possibility is that the CO binds to $CO_2$ or CO rather than the Ru surface.

In our case, the surface coverage is rather low, making the latter case rather unlikely. Furthermore, as can be seen below, there is no evidence that the oxygen dissociation product chemisorbs stably to ruthenium. Therefore, we propose that the CO adsorbs at two different sites with two different binding energies, possibly due to the proximity of $CO_2$. Only the higher energy vibrational mode is strongly dependent on the concentration of $CO_2$, which might be associated with the strengthening of the C−O bond (peak at 1996 $cm^{-1}$) and a weakening of the bond between the surface and CO (peak at 1983 $cm^{-1}$).[32]

**3.3. CO Adsorption from the Residual Background Gases on Ru(0001).** To avoid mistaking $CO_2$ partial dissociation for CO adsorption from background, the adsorption of CO from the background was measured. After cleaning the Ru(0001) surface, the surface was flashed to 600 K to remove any residual CO. The sample was then cooled to 85 K, and RAIRS measurements were performed after delays of 25 and 50 min (see Figure 7). A peak at 1990 $cm^{-1}$, corresponding to CO adsorbed

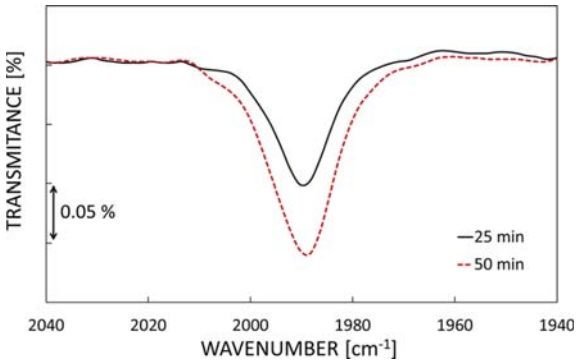


**Figure 7.** Background CO adsorption on Ru(0001) surface after 25 and 50 min of delay at a temperature of 85 K.

to the surface, is observed.[28] It can be seen that the peak increases with time. Moreover, a slight red-shift from 1990 to 1988 $cm^{-1}$ is observed.

To estimate the amount of CO adsorbing on the surface, TPD measurements were performed under the same conditions. TPD was performed immediately after the surface was cooled to 85 K and after delays of 25 and 50 min after heating to 600 K and cooling to 85 K. As shown in Figure 8, the TPD spectrum showed that the surface coverage of $H_2$, $H_2O$, and CO (Figure 8a−c, respectively) increases with time.

The surface coverage of CO, $H_2$, and $H_2O$ due to background gases is presented in Figure 9. There is no significant amount of water on the clean sample, but after exposing to ambient for 50 min, the amount of water increased to approximately 0.004 of a monolayer. A small amount of CO (0.001 ML) deposits onto the surface very quickly (faster than water), but only grows slowly (8 times slower than water) after that. Hydrogen grows fastest, from 0.003 to 0.017 ML. A comparison between the growth of the CO peak after $CO_2$ dosing with the growth of CO from background is presented on Figure 10 and in Table 2.

It is clear that the CO peak grows four times more on a surface that is dosed with $CO_2$ compared to the natural adsorption from background gases. Furthermore, it can be seen from Figure 5 that the growth of the CO peak corresponds very well to the decay of the $CO_2$ peak. This suggests that desorption of $CO_2$ at 85 K is rather slow and that the changes in the infrared spectra are dominated by partial dissociation. After $CO_2$ dosing onto the surface, two CO peaks at different positions are observed, which is indicative of a low and high energy binding site. To determine the stability of those peaks, the surface was annealed above the temperature of the main desorption peak of $CO_2$. As stated earlier, the Ru(0001) surface was dosed with $CO_2$ (1 mbar, 10 min) and, after 50 min, was heated to 120 K. After cooling to 85 K, a RAIRS spectrum was obtained (see Figure 11).



DOI: 10.1021/acs.jpcc.7b00021
J. Phys. Chem. C XXXX, XXX, XXX−XXX

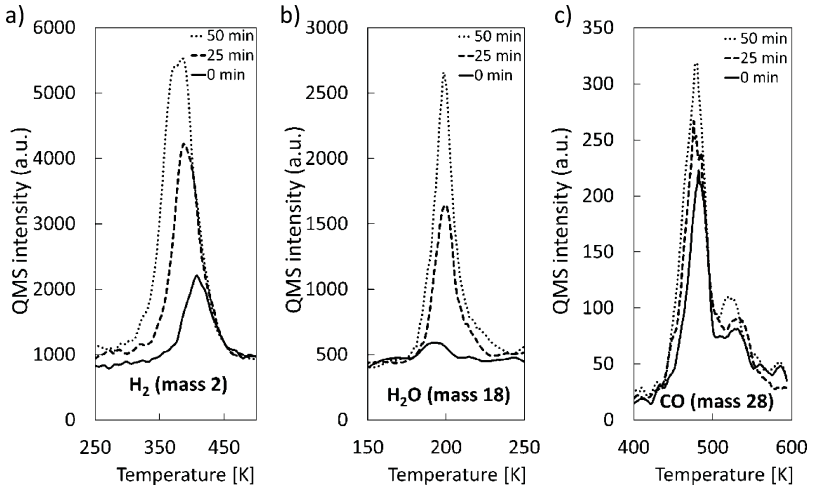


**Figure 8.** TPD of (a) $H_2$, (b) $H_2O$, and (c) CO adsorbed from residual background at a sample temperature of 85 K. No other masses detected.

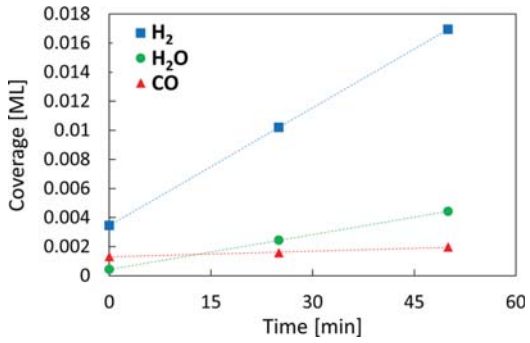


**Figure 9.** Surface coverage of CO, $H_2O$, and $H_2$ on Ru(0001) due to background gases.

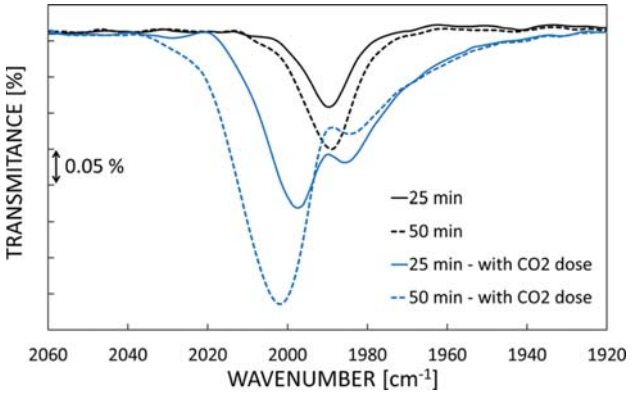


**Figure 10.** Comparison of the reflection−absorption infrared spectrum of CO peak, from the residual background gases and CO peak after $CO_2$ dosing, after 25 and 50 min delay.

**Table 2. CO Surface Coverage in ML from the Background Residual Gases and after $CO_2$ Dose onto the Surface**

| | CO surface coverage in ML | |
|---|---|---|
| time (min) | background | with $CO_2$ dose |
| 25 | 0.0016 | 0.005 |
| 50 | 0.002 | 0.008 |

Table 3 shows that the $CO_2$ coverage is reduced by a factor of 2. Complete desorption is not achieved because, as can be seen

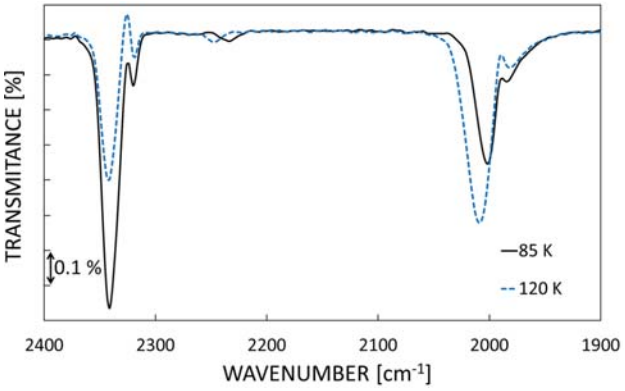


**Figure 11.** Reflection−absorption infrared spectrum after 10 min $CO_2$ (1 mbar) dosing onto the Ru(0001) and 50 min delay time on Ru(0001) single crystal at 85 K and after sample annealing to 120 K.

**Table 3. Surface Coverage of CO and $CO_2$ (after $CO_2$ Dose onto the Ru(0001) Surface 50 min Delay) at 85 K and after Annealing to 120 K**

| | indicative surface coverage in ML | |
|---|---|---|
| temp (K) | CO | $CO_2$ |
| 85 | 0.01 | 0.028 |
| 120 | 0.016 | 0.014 |

in Figure 2, the $CO_2$ desorption spectrum has a peak at 105 K, followed by a broad feature that extends beyond 120 K. The surface coverage of CO increases from 0.01 to 0.016 of a ML. Interestingly, the overall increase is accompanied by a 23% reduction in the lower energy peak and a 65% increase in the higher energy peak. In addition to changes in peak intensity, after annealing, the peak positions also change slightly. The higher energy peak blue-shifts from 2002 to 2010 $cm^{-1}$, and the lower energy peak red-shifts from 1984 to 1980 $cm^{-1}$. Both shifts are likely to be due to coverage-dependent effects.[29]

**3.4. Oxygen TPD.** A remaining question relates to the oxygen radical. Since the generated amount of CO is very low, it is possible that the oxygen atoms are consumed for forming CO with residual carbon in the crystal. This should then give a small CO desorption at high temperature, which may be difficult to detect in such small doses. Another option is that oxygen can


DOI: 10.1021/acs.jpcc.7b00021
J. Phys. Chem. C XXXX, XXX, XXX−XXX

form water with background $H_2$. Formation of such small amounts of water is not detectable due to presence of background water in the TPD spectrum. Our RAIRS measurements were unable to reliably detect an increase in the OH stretch mode, but it should be noted that RAIRS is generally not able to detect submonolayer amounts of water since the first monolayer of water on Ru does not have a significant dipole moment perpendicular to the surface.[33] A third possibility is that the oxygen chemisorbs with the ruthenium surface. To find the role of oxygen chemisorption, the oxygen signal was always recorded in TPD after $CO_2$ adsorption. However, no significant signal at 1580 K was detected, indicating that ruthenium oxide is not formed during $CO_2$ dissociation or that the oxygen is consumed for forming CO from residual carbon that diffuses out of the bulk of the crystal at high temperature.

Furthermore, we also exclude reassociation due to $CO_2 \underset{k_2}{\overset{k_1}{\rightleftarrows}} CO + O$, with $k_1 \approx k_2$. If this were the case, then, after annealing the ruthenium and removing the majority of $CO_2$, the surface concentrations would be out of equilibrium and favor the reverse reaction. However, neither an increase in $CO_2$ nor a decrease in the CO vibrational mode intensity is observed. This implies that $k_1 \gg k_2$. Finally, the reassociation during TPD can also be excluded because there is no evidence for a significant $CO_2$ desorption peak at the CO desorption temperature.

## 4. CONCLUSIONS

Our results show that $CO_2$ adsorption on a Ru(0001) surface results in partial dissociation, with $CO_2$ and CO present on the surface. RAIRS measurements show that $CO_2$ dissociates into CO over time. For a $CO_2$ coverage of 0.05 ML, dissociation proceeds to a $CO_2$ coverage of 0.03 ML and appears to saturate. Furthermore, the dissociation of $CO_2$ appears to be irreversible. In comparison with previous results reported for Ni(110),[18,30] and Fe(111),[9,19,34,35] we note that the dissociation of $CO_2$ is qualitatively similar, but has some significant differences. For both Ni and Fe, partial dissociation is only observed for elevated temperatures, while for Ru(0001), dissociation is already observed at 85 K. Furthermore, in the case of Ni and Fe, the oxygen is observed to be adsorbed to the surface, while for Ru, there is no evidence of O adsorption. Finally, on further heating, CO decomposes into carbon and oxygen on Fe, while on Ru, CO desorbs intact. Observed vibrational modes at 660 and 2343 $cm^{-1}$ correspond to stretch modes of linear, undisturbed $CO_2$, while a vibrational feature that is visible only for higher $CO_2$ coverages at 1580 $cm^{-1}$ is tentatively assigned to an asymmetric stretching mode of a bent $CO_2$ species.

The adsorption ($CO_2$ does not adsorb for temperatures higher than 100 K) and desorption temperatures of $CO_2$ on Ru are relatively low in comparison to those reported for other transition metals.[1] By annealing the surface at 120 K, just above the peak desorption temperature of $CO_2$, it was observed that the rate of $CO_2$ dissociation was increased and that the CO restructures to a weaker bond between the surface and CO. TPD spectra confirm that the changes in the RAIRS spectrum are due to changes in CO and $CO_2$ coverage. Furthermore, TPD does not show chemisorbed oxygen on the Ru surface, which may be due to $H_2O$ or CO formation from residual $H_2$ or C on the sample.

## AUTHOR INFORMATION


### Corresponding Author

*E-mail: c.j.lee@utwente.nl.

### ORCID

M. Pachecka: 0000-0002-2323-7954


### Notes

The authors declare no competing financial interest.

## ACKNOWLEDGMENTS

This work is supported by NanoNextNL, a micro and nanotechnology consortium of the Government of The Netherlands and 130 partners. We acknowledge the support of ASML, Carl Zeiss SMT AG, PANalytical, SolMates, TNO, and Demcon, as well as the Province of Overijssel and the Foundation FOM. This work is additionally supported by the research programme Controlling Photon and Plasma Induced Processes at EUV Optical Surfaces (CP3E) of the Stichting voor Fundamenteel Onderzoek der Materie (FOM) with financial support from the Nederlandse Organisatie voor Wetenschappelijk Onderzoek (NWO). The authors would like to thank Mr. Feng Liu, Mr. Goran Milinkovic, and Mr. John de Kuster for the technical support.

## REFERENCES


(1) Solymosi, F. The Bonding, Structure and Reactions of Co2 Adsorbed on Clean and Promoted Metal Surfaces. *J. Mol. Catal.* **1991**, *65*, 337−358.

(2) Kuhl, K. P.; Hatsukade, T.; Cave, E. R.; Abram, D. N.; Kibsgaard, J.; Jaramillo, T. F. Electrocatalytic Conversion of Carbon Dioxide to Methane and Methanol on Transition Metal Surfaces. *J. Am. Chem. Soc.* **2014**, *136*, 14107−14113.

(3) Wang, Y.; Lafosse, A.; Jacobi, K. Adsorption and Reaction of Co2 on the Ruo2(110) Surface. *J. Phys. Chem. B* **2002**, *106*, 5476−5482.

(4) Mark, M. F.; Maier, W. F. Co2-Reforming of Methane on Supported Rh and Ir Catalysts. *J. Catal.* **1996**, *164*, 122−130.

(5) Utaka, T.; Okanishi, T.; Takeguchi, T.; Kikuchi, R.; Eguchi, K. Water Gas Shift Reaction of Reformed Fuel over Supported Ru Catalysts. *Appl. Catal., A* **2003**, *245*, 343−351.

(6) Bricker, J. C.; Nagel, C. C.; Shore, S. G. Reactivities of Ruthenium Cluster Anions: Implications for Catalysis of the Water-Gas Shift Reaction. *J. Am. Chem. Soc.* **1982**, *104*, 1444−1445.

(7) Graves, C.; Ebbesen, S. D.; Mogensen, M.; Lackner, K. S. Sustainable Hydrocarbon Fuels by Recycling Co2 and H2o with Renewable or Nuclear Energy. *Renewable Sustainable Energy Rev.* **2011**, *15*, 1−23.

(8) Zhao, P.; He, Y.; Cao, D. B.; Wen, X.; Xiang, H.; Li, Y. W.; Wang, J.; Jiao, H. High Coverage Adsorption and Co-Adsorption of Co and H2 on Ru(0001) from Dft and Thermodynamics. *Phys. Chem. Chem. Phys.* **2015**, *17*, 19446−19456.

(9) Freund, H. J.; Gehner, H.; Bartos, B.; Wedler, G. Co2 Adsorption and Reaction on Fe(111): And Angle Resolved Photoemission (Arups) Study. *Surf. Sci.* **1987**, *180*, 550−564.

(10) McCarty, J.; Falconer, J.; Madix, R. J. Decomposition of Formic Acid on Ni(L10) I.Flash Decomposition from the Clean Surface and Flash Desorption of Reaction Products. *J. Catal.* **1973**, *30*, 235−249.

(11) Benziger, J. B.; Madix, R. J. The Decomposition of Formic Acid on Ni (100). *Surf. Sci.* **1979**, *79*, 394−412.

(12) Asscher, M.; Kao, C. T.; Samorjai, G. A. High-Resolution Electron Energy Loss Spectroscopic Study of Co2, Adsorbed on Re(0001). *J. Phys. Chem.* **1988**, *92*, 2711−2714.

(13) Carley, A. F.; Gallagher, D. E.; Roberts, M. W. Activation of Carbon Dioxide at Low Temperatures at Aluminium Surfaces. *Surf. Sci.* **1987**, *183*, 263−268.

(14) Eren, B.; Zherebetskyy, D.; Patera, L. L.; Wu, C. H.; Bluhm, H.; Africh, C.; Wang, L.-W.; Somorjai, G. A.; Salmeron, M. Activation of Cu(111) Surface by Decomposition into Nanoclusters Driven by Co Adsorption. *Science* **2016**, *351*, 475−478.




DOI: 10.1021/acs.jpcc.7b00021
J. Phys. Chem. C XXXX, XXX, XXX−XXX

(15) Mongeot; de, F. B.; Scherer, M.; Gleich, B.; Kopatzki, E.; Behm, R. J. Co Adsorption and Oxidation on Bimetallic Pt/Ru(0001) Surfaces − a Combined Stm and Tpd/Tpr Study. *Surf. Sci.* **1998**, *411*, 249−262.
(16) Onishi, H.; Iwasawa, Y. Reconstruction of Tio,(110) Surface: Stm Study with Atomic-Scale Resolution. *Surf. Sci.* **1994**, *313*, 783−789.
(17) Kong, D.; Zhu, J.; Ernst, K.-H. Low-Temperature Dissociation of Co2 on a Ni/Ceo2(111)/Ru(0001) Model Catalyst. *J. Phys. Chem. C* **2016**, *120*, 5980−5987.
(18) Wambach, J.; Illing, G.; Freund, H. J. Co2 Activation and Reaction with Hydrogen on Ni (110): Formate Formation. *Chem. Phys. Lett.* **1991**, *184*, 239−244.
(19) Behner, H.; Spiess, W.; Wedler, G.; Borgmann, D.; Freund, H. J. Electron Energy Loss Study of the Electronically Excited States of Adsorbedco2: Case Study Co2/Fe. *Surf. Sci.* **1987**, *184*, 335−344.
(20) Diemant, T.; Schuttler, K. M.; Behm, R. J. Ag on Pt(111): Changes in Electronic and Co Adsorption Properties Upon Ptag/Pt(111) Monolayer Surface Alloy Formation. *ChemPhysChem* **2015**, *16*, 2943−2952.
(21) Wang, W.; Li, L.; Zhou, Q.; Pan, J.; Zhang, Z. L.; Tok, E. S.; Yeo, Y.-C. Tin Surface Segregation, Desorption, and Island Formation During Post-Growth Annealing of Strained Epitaxial Ge1−Xsnx Layer on Ge(001) Substrate. *Appl. Surf. Sci.* **2014**, *321*, 240−244.
(22) Böttcher, A.; Niehus, H. Formation of Subsurface Oxygen at Ru(0001). *J. Chem. Phys.* **1999**, *110*, 3186−3195.
(23) Madey, T. E.; Faradzhev, N. S.; Yakshinskiy, B. V.; Edwards, N. V. Surface Phenomena Related to Mirror Degradation in Extreme Ultraviolet (Euv) Lithography. *Appl. Surf. Sci.* **2006**, *253*, 1691−1708.
(24) Gerakines, P. A.; Schutte, W. A.; Greenberg, J. M.; Dishoeck van, E. F. The Infrared Band Strengths of H2o, Co and Co2 in Laboratory Simulations of Astrophysical Ice Mixtures. *Astron. Astrophys.* **1995**, *296*, 810−818.
(25) Smith, A. L. *The Coblentz Society Desk Book of Infrared Spectra*, 2nd ed.; Coblentz Society, 1982.
(26) Liu, Z. M.; Zhou, Y.; Solymosi, F.; White, J. M. Spectroscopic Study of K-Induced Activation of Co, on Pt(111). *Surf. Sci.* **1990**, *245*, 289−304.
(27) Liu, Z. M.; Zhou, Y.; Solymosi, F.; White, J. M. Vibrational Study of Co2- on K-Promoted Pt(111). *J. Phys. Chem.* **1989**, *93*, 4383−4385.
(28) Liu, F.; Sturm, J. M.; Lee, C. J.; Bijkerk, F. Extreme Uv Induced Dissociation of Amorphous Solid Water and Crystalline Water Bilayers on Ru(0001). *Surf. Sci.* **2016**, *646*, 101−107.
(29) Pfnür, H.; Menzel, D. High Resolution Vibrational Spectroscopy of Co on Ru(Oo1): The Importance of Lateral Interactions. *Surf. Sci.* **1980**, *93*, 431−452.
(30) Bartos, B.; Freund, H. J. Adsorption and Reaction of Co, and Co,/0 Co-Adsorption on Ni(110): Angle Resolved Photoemission (Arups) and Electron Energy Loss (Hreels) Studies. *Surf. Sci.* **1987**, *179*, 59−89.
(31) Collins, A. C.; Trapnell, B. M. W. Co2 Chemisorption on Evaporated Metal Films. *Trans. Faraday Soc.* **1957**, *53*, 1476−1482.
(32) Zeinalipour-Yazdi, C. D.; Willock, D. J.; Thomas, L.; Wilson, K.; Lee, A. F. Co Adsorption over Pd Nanoparticles: A General Framework for Ir Simulations on Nanoparticles. *Surf. Sci.* **2016**, *646*, 210−220.
(33) Clay, C.; Haq, S.; Hodgson, A. Intact and Dissociative Adsorption of Water on Ru(0001). *Chem. Phys. Lett.* **2004**, *388*, 89−93.
(34) Behner, H.; Spiess, W.; Wedler, G.; Dorgmann, D. Interaction of Carbon Dioxide with Fe(110), Stepped Fe(110) and Fe(111). *Surf. Sci.* **1986**, *175*, 276−286.
(35) Yoshida, K.; Samorjai, G. A. The Chemisorption of Co, Co2, C2h2, C2h4, H2 and Nh3 on the Clean Fe(100) and (111) Crystal Surfaces. *Surf. Sci.* **1978**, *75*, 46−60.



DOI: 10.1021/acs.jpcc.7b00021
*J. Phys. Chem. C* XXXX, XXX, XXX−XXX